Subtracted Second RPA and Lee-Suzuki -Okamoto similarity transformation

DFT2025, March 25-27, Kobe, Japan

Fundamentals, Developments and Applications

H. Sagawa (RIKEN/University of Aizu/ITP, CAS)

1. Introduction
2. **Subtracted Second RPA and Lee-Suzuki-Okamoto similarity transformation**
3. SSRPA for M1 excitations for doubly closed-shell nuclei
4. SSRPA for Gamow-Teller resonances
5. RPA and SSRPA for beta-decay
6. Summary

RIKEN NISHINA CENTER

THE UNIVERSITY OF AIZU
to Advance Knowledge for Humanity · 1993 ·

Beyond mean field model (Subtracted Second RPA) with EDF

Targets of Second RPA

Giant Resonances
Gamow-Teller states
beta decay

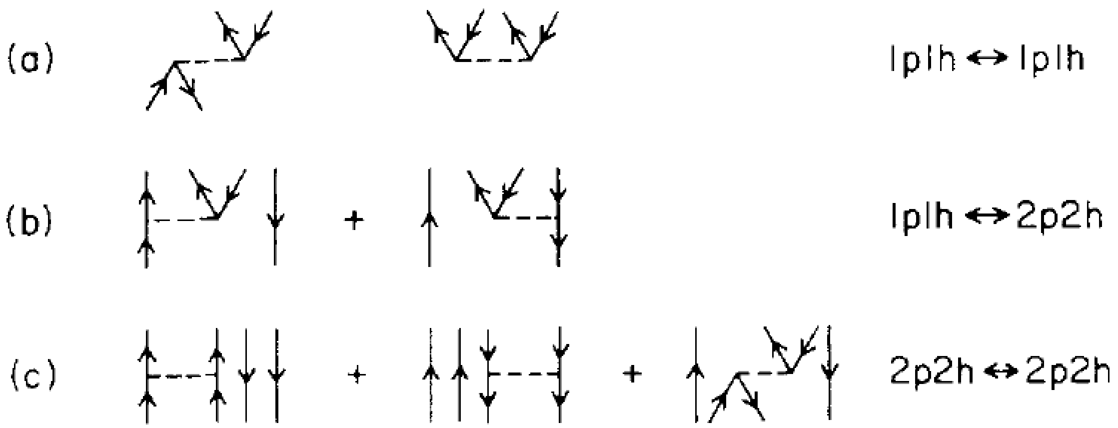

- More correlations in Collective and non-collective excitations
  - 1p-1h+2p+2h correlations
  - tensor correlations
  - Pairing correlations
    - keeping universality of applications

- Spreading width of giant resonances
- Quenching of spin-isospin excitations.
- Low-energy pigmy states
- Beta-decay lifetime

RPA (random phase approximation) and SSRPA (subtracted second RPA) models

RPA ground state is defined as

$$|\Psi\rangle = e^{\hat{S}}|\Phi\rangle,$$

where

$$\hat{S} = \sum_{ph} C_{ph}(t) a_p^\dagger a_h,$$

SRPA operator is

$$\hat{S} = \sum_{ph} C_{ph}(t) a_p^\dagger a_h + \frac{1}{2} \sum_{php'h'} \hat{C}_{pp'hh'}(t) a_p^\dagger a_{p'}^\dagger a_h a_{h'}.$$

The basic idea is the same as the coupled cluster model with singlet (s)- and doublet (d)- pairs.

SRPA phonon operator

$$Q_\nu^\dagger = \sum_{ph} (X_{ph}^\nu a_p^\dagger a_h - Y_{ph}^\nu a_h^\dagger a_p)$$

RPA

$$+ \sum_{\substack{p_1<p_2 \\ h_1<h_2}} (X_{p_1p_2h_1h_2}^\nu a_{p_1}^\dagger a_{p_2}^\dagger a_{h_2} a_{h_1} - Y_{p_1p_2h_1h_2}^\nu a_{h_1}^\dagger a_{h_2}^\dagger a_{p_2} a_{p_1})$$

SRPA

Equation of motion gives SRPA matrix equation

$$[H, Q^\dagger] = \hbar\omega Q^\dagger$$

RPA equation.

$$\begin{bmatrix} A & B \\ -B^* & -A^* \end{bmatrix} \begin{bmatrix} X^\nu \\ Y^\nu \end{bmatrix} = \hbar\omega_\nu \begin{bmatrix} X^\nu \\ Y^\nu \end{bmatrix}$$

(a)  1p1h ↔ 1p1h

$$\begin{aligned} A_{11} =& A_{ph;p'h'} \\ =& < HF|[a_h^\dagger a_p, [H, a_{p'}^\dagger a_{h'}]]|HF > \\ =& (E_p - E_h)\delta_{pp'}\delta_{hh'} + \bar{V}_{ph'hp'} \end{aligned}$$

$$\begin{aligned} B_{11} =& B_{ph;p'h'} \\ =& - < HF|[a_h^\dagger a_p, [H, a_{h'}^\dagger a_{p'}]]|HF > \\ =& \bar{V}_{pp'hh'} \end{aligned}$$

RPA equation.

$$\begin{bmatrix} A & B \\ -B^* & -A^* \end{bmatrix} \begin{bmatrix} X^\nu \\ Y^\nu \end{bmatrix} = \hbar\omega_\nu \begin{bmatrix} X^\nu \\ Y^\nu \end{bmatrix}$$

$$A = \begin{pmatrix} A_{11} & A_{12} \\ A_{21} & A_{22} \end{pmatrix}, B = \begin{pmatrix} B_{11} & B_{12} \\ B_{21} & B_{22} \end{pmatrix}$$

$$X = \begin{pmatrix} X_1^\nu \\ X_2^\nu \end{pmatrix}, Y = \begin{pmatrix} Y_1^\nu \\ Y_2^\nu \end{pmatrix}$$

$$\begin{aligned} A_{11} =& A_{ph;p'h'} \\ =& < HF|[a_h^\dagger a_p, [H, a_{p'}^\dagger a_{h'}]]|HF > \\ =& (E_p - E_h)\delta_{pp'}\delta_{hh'} + \bar{V}_{ph'hp'} \end{aligned}$$

$$\begin{aligned} B_{11} =& B_{ph;p'h'} \\ =& - < HF|[a_h^\dagger a_p, [H, a_{h'}^\dagger a_{p'}]]|HF > \\ =& \bar{V}_{pp'hh'} \end{aligned}$$

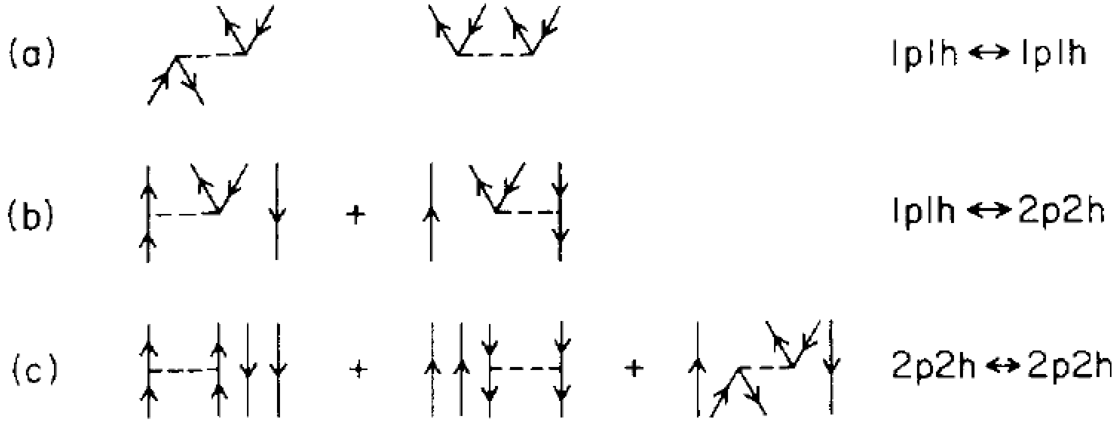

$$\begin{aligned} A_{12} =& A_{ph;p_1p_2h_1h_2} \\ =& < HF|[a_h^\dagger a_p, [H, a_{p_1}^\dagger a_{p_2}^\dagger a_{h_2} a_{h_1}]]|HF > \\ =& U(h_1h_2)\bar{V}_{p_1p_2ph_2}\delta_{hh_1} - U(p_1p_2)\bar{V}_{hp_2h_1h_2}\delta_{pp_1} \end{aligned}$$

$U(h_1h_2)$ is an anti-symmtrizer.

$$\begin{aligned} A_{22} =& A_{p_1p_2h_1h_2;p_1'p_2'h_1'h_2'} \\ =& < HF|[a_{h_1}^\dagger a_{h_2}^\dagger a_{p_2} a_{p_1}, [H, a_{p_1'}^\dagger a_{p_2'}^\dagger a_{h_2'} a_{h_1'}]]|HF > \\ =& (E_{p_1} + E_{p_2} - E_{h_1} - E_{h_2})U(p_1p_2)U(h_1h_2) \\ & \times \delta_{p_1p_1'}\delta_{p_2p_2'}\delta_{h_1h_1'}\delta_{h_2h_2'} \\ & + U(h_1h_2)\bar{V}_{p_1p_2p_1'p_2'}\delta_{h_1h_1'}\delta_{h_2h_2'} \\ & + U(p_1p_2)\bar{V}_{h_1h_2h_1'h_2'}\delta_{p_1p_1'}\delta_{p_2p_2'} \\ & - U(p_1p_2)U(h_1h_2)U(p_1'p_2')U(h_1'h_2') \\ & \times \bar{V}_{p_1h_1'p_1'h_1}\delta_{p_2p_2'}\delta_{h_2h_2'} \end{aligned}$$

The Subtraction procedure

Large scale SRPA calculations have shown that:

- The SRPA strength distribution is sistematically shifted towards lower energies compared to the RPA one
- This shift is very strong ($\simeq$ 3-4 MeV), RPA description often spoiled

This is trivial since EDF is designed to describe the mean field properties of nuclear observables; in other words for HF and RPA calculations

The Subtraction procedure (I. Tselyaev Phys. Rev. C 75, 024306 (2007))

- Designed for beyond RPA approaches
- It restores the Thouless theorem, e.g. instabilities are removed
- Static ($\omega = 0$) limit of the SRPA imposed to be equal to the RPA one

SRPA=> convert to RPA-like eqation

SRPA ->Energy dependent RPA-like equation

$$A_{11'}(\omega) = A_{11'} + \sum_{2,2'} A_{12}(\omega + i\eta - A_{22'})^{-1} A_{2'1'} - \sum_{2,2'} B_{12}(\omega + i\eta + A_{22'})^{-1} B_{2'1'},$$

$$B_{11'}(\omega) = B_{11'} + \sum_{2,2'} A_{12}(\omega + i\eta - A_{22'})^{-1} B_{2'1'} - \sum_{2,2'} B_{12}(\omega + i\eta + A_{22'})^{-1} A_{2'1'}. \qquad (11)$$

Subtraction matrix

(If we subtract $E_{11'}(\omega = 0)$ *and* $F(\omega = 0)$ *from* A *and* B,

$SRPA(\omega = 0) = RPA$

$$E_{11'}(\omega) = \sum_{2,2'} A_{12}(\omega + i\eta - A_{22'})^{-1} A_{2'1'} - \sum_{2,2'} B_{12}(\omega + i\eta + A_{22'})^{-1} B_{2'1'},$$

$$F_{11'}(\omega) = \sum_{2,2'} A_{12}(\omega + i\eta - A_{22'})^{-1} B_{2'1'} - \sum_{2,2'} B_{12}(\omega + i\eta + A_{22'})^{-1} A_{2'1'}.$$

$$A^S_{11'}(\omega) = A_{11'}(\omega) - E_{11'}(0),$$

$$B^S_{11'}(\omega) = B_{11'}(\omega) - F_{11'}(0).$$

In SRPA with subtraction procedure (SSRPA), A_{11} and B_{11} are modified.

$$A^S_{11'} = A_{11'} + \sum_2 A_{12}(A_{22})^{-1}A_{21'} + \sum_2 B_{12}(A_{22})^{-1}B_{21'}$$

$$B^S_{11'} = B_{11'} + \sum_2 A_{12}(A_{22})^{-1}B_{21'} + \sum_2 B_{12}(A_{22})^{-1}A_{21'}$$

$A_{ph,p'h'}(E) =$

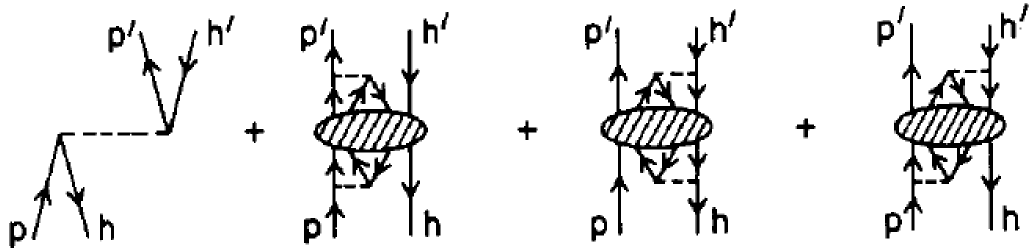

Energy independent SSRPA equation

$$\mathcal{A}^S_F = \begin{pmatrix} A_{11'} + \sum_{2,2'} A_{12}(A_{22'})^{-1}A_{2'1'} + \sum_{2,2'} B_{12}(A_{22'})^{-1}B_{2'1'} & A_{12} \\ A_{21} & A_{22'} \end{pmatrix},$$

$$\mathcal{B}^S_F = \begin{pmatrix} B_{11'} + \sum_{2,2'} A_{12}(A_{22'})^{-1}B_{2'1'} + \sum_{2,2'} B_{12}(A_{22'})^{-1}A_{2'1'} & B_{12} \\ B_{21} & 0 \end{pmatrix}.$$

Lee-Suzuki-Okamoto similarity transformation

Lee and Suzuki, Prog. Theor. Phys. 64 (1980)
Suzuki and Okamoto, Prog. Theor. Phys. 92, 1045 (1994)

Consider $|\Phi_\nu\rangle$ is a complete set of eigenstates of H,

Dream

$$H|\Phi_\nu\rangle = E_\nu|\Phi_\nu\rangle. \tag{3.208}$$

Each state $|\Phi_\nu\rangle$ is decomposed into the P and Q spaces as

Reality

$$|\Phi_\nu\rangle = (P+Q)|\Phi_\nu\rangle = |\nu\rangle + Q|\Phi_\nu\rangle \tag{3.209}$$

where $|\nu\rangle \equiv P|\Phi_\nu\rangle$. Define the operator S which maps the state in Q space into P space

$$S|\nu\rangle = Q|\Phi_\nu\rangle. \tag{3.210}$$

Then, we have

$$|\Phi_\nu\rangle = (I+S)|\nu\rangle \tag{3.211}$$

where I is the identity operator. The operator S satisfies the relations,

$$QSP = S, \quad PSP = QSQ = 0, \quad S^2 = 0. \tag{3.212}$$

Thus, the operator e^{+S} has the inverse e^{-S} being a unitary operator, which makes possible the mapping,

$$|\Phi_\nu\rangle = e^S|\nu\rangle, \quad |\nu\rangle = e^{-S}|\Phi_\nu\rangle. \qquad (3.214)$$

Similarity transformation

These mappings are called "similarity transformations". Then, $|\nu\rangle$ is an eigenstate of a Hamiltonian

$$H_S = e^{-S}He^S, \qquad (3.215)$$

with the eigenvalue E_ν since

$$\langle\Phi_\nu|H|\Phi_\nu\rangle = \langle\Phi_\nu|e^S e^{-S}He^S e^{-S}|\Phi_\nu\rangle = \langle\nu|H_S|\nu\rangle = E_\nu. \qquad (3.216)$$

The decoupling condition

$$QH_SP = Qe^{-S}He^SP = 0,$$

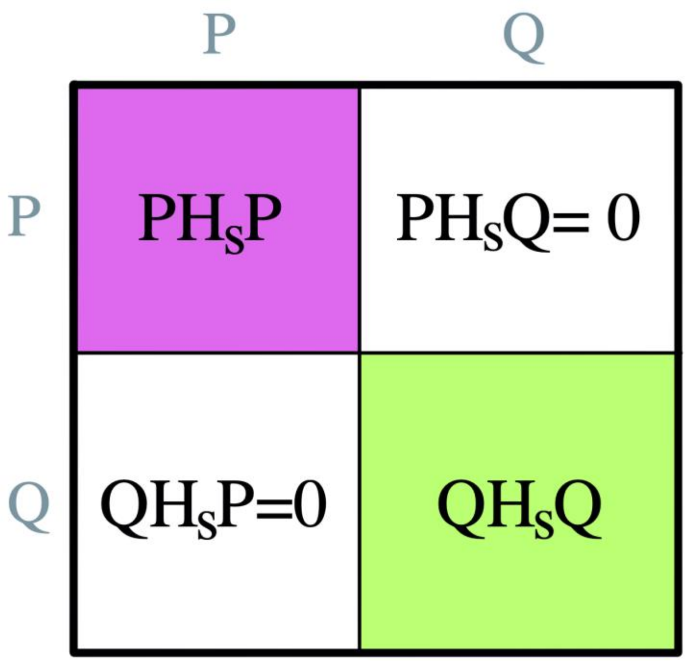

The effective Hamiltonian H_P in the model space P is expanded to be

$$H_S = e^{-S}He^S = H + [H, S] + \frac{1}{2}[[H, S], S] + \cdots. \qquad (3.218)$$

In general, the commutator terms contain two-, three-, $\cdots$, A-body operators, i.e., the Hamiltonian H_S can be written in a cluster expansion form as

$$H_S = \mathcal{H}^{(1)} + \mathcal{H}^{(2)} + \mathcal{H}^{(3)} + \cdots, \qquad (3.219)$$

S_{12} is an operator to map Q-space to P-space

With the condition of Eq. (3.217), the operator S_{12} can be expressed as

$$S_{12} = \tanh^{-1}(\omega - \omega^{\dagger}), \tag{3.220}$$

with the operator

$$\omega = \sum_{k=1}^{d} Q|\Phi_k\rangle\langle\tilde{\phi}_k|P, \tag{3.221}$$

of the P space. The effective interaction is then given by

$$R = H_{\text{eff}} - PH_0P = PVP + \sum_{\mu=1}^{d} PVQ \frac{1}{E_\mu - QHQ} QVP|\phi_\mu\rangle\langle\tilde{\phi}_\mu| . \tag{2·24}$$

The true eigenstate of H corresponding to the P-space eigenstate $|\phi_\mu\rangle$ is given by

$$|\Psi_\mu\rangle = e^\omega|\phi_\mu\rangle$$

$$= |\phi_\mu\rangle + \omega(E_\mu)|\phi_\mu\rangle. \tag{2·25}$$

The P-space eigenvalue problem is then written as

$$H_{\text{eff}}|\phi_\mu\rangle = (PH_0P + R)|\phi_\mu\rangle = E_\mu|\phi_\mu\rangle .$$

PH_0P+R=>EDF

The eigenvalue E_μ agrees with one of the eigenvalues of H, as long as ω is a solution to Eq. (2·19). In terms of E_μ and $|\phi_\mu\rangle$, Eq. (2·19) can be solved formally as

$$\omega = \sum_{\mu=1}^{d} \omega(E_\mu)|\phi_\mu\rangle\langle\tilde{\phi}_\mu| \tag{2·22}$$

with

$$\omega(E_\mu) = \frac{1}{E_\mu - QHQ} QVP , \tag{2·23}$$

In SRPA with subtraction procedure (SSRPA), A_{11} and B_{11} are modified.

$$A^S_{11'} = A_{11'} + \sum_2 A_{12}(A_{22})^{-1}A_{21'} + \sum_2 B_{12}(A_{22})^{-1}B_{21'}$$

$$B^S_{11'} = B_{11'} + \sum_2 A_{12}(A_{22})^{-1}B_{21'} + \sum_2 B_{12}(A_{22})^{-1}A_{21'}$$

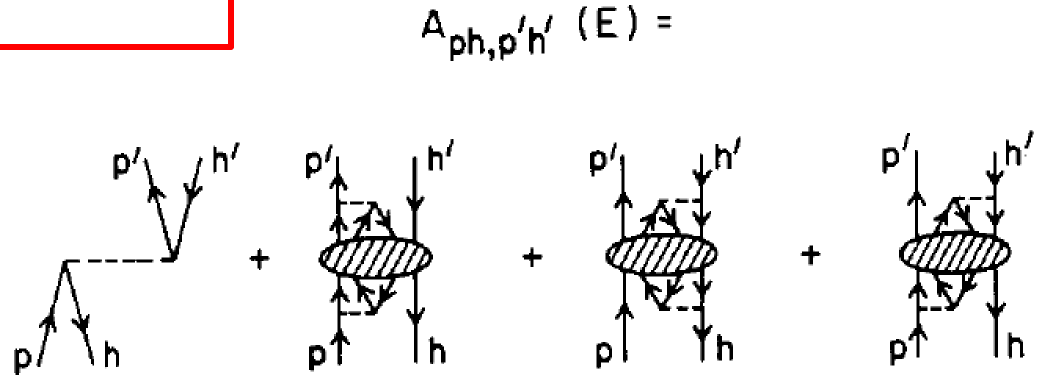

Energy independent SSRPA equation

$$\mathcal{A}^S_F = \begin{pmatrix} A_{11'} + \sum_{2,2'} A_{12}(A_{22'})^{-1}A_{2'1'} + \sum_{2,2'} B_{12}(A_{22'})^{-1}B_{2'1'} & A_{12} \\ A_{21} & A_{22'} \end{pmatrix},$$

$$\mathcal{B}^S_F = \begin{pmatrix} B_{11'} + \sum_{2,2'} A_{12}(A_{22'})^{-1}B_{2'1'} + \sum_{2,2'} B_{12}(A_{22'})^{-1}A_{2'1'} & B_{12} \\ B_{21} & 0 \end{pmatrix}.$$

Similarity Renormalization Group (SRG)

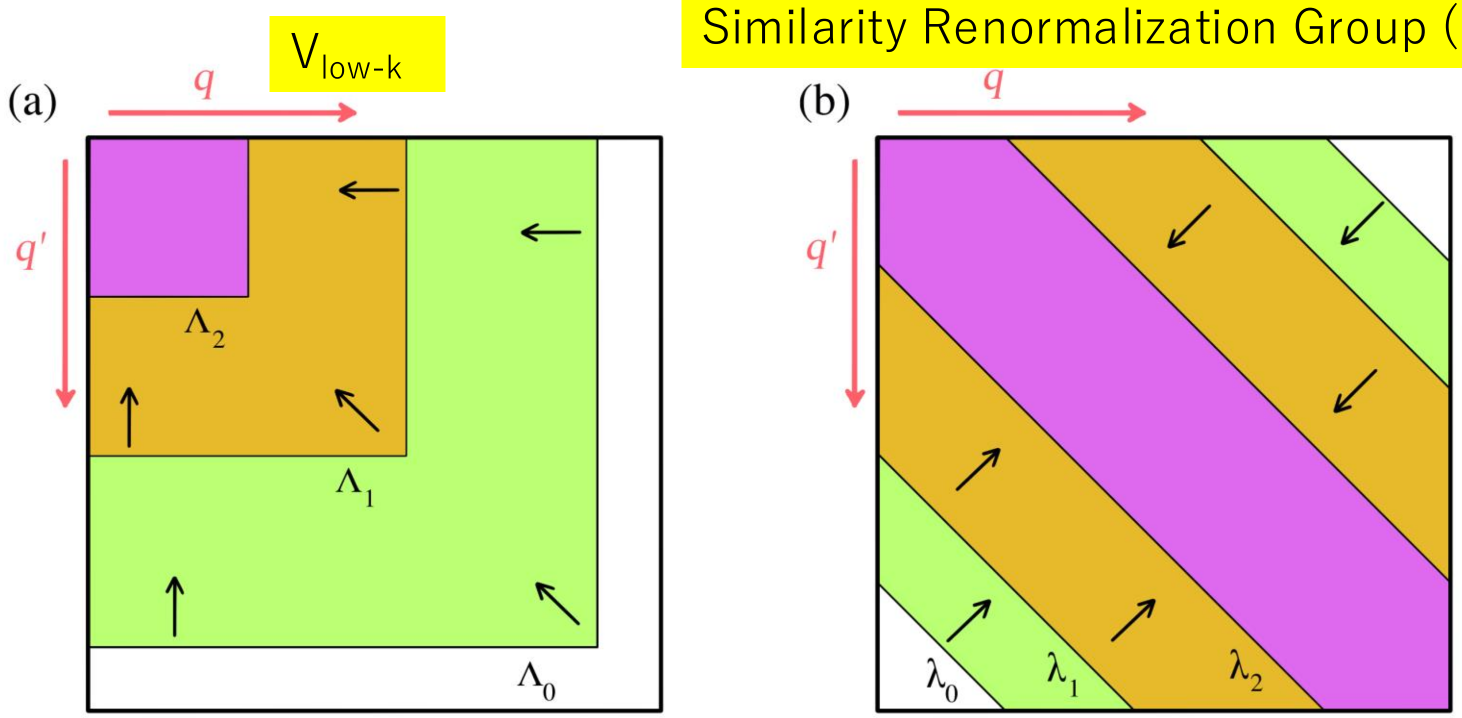

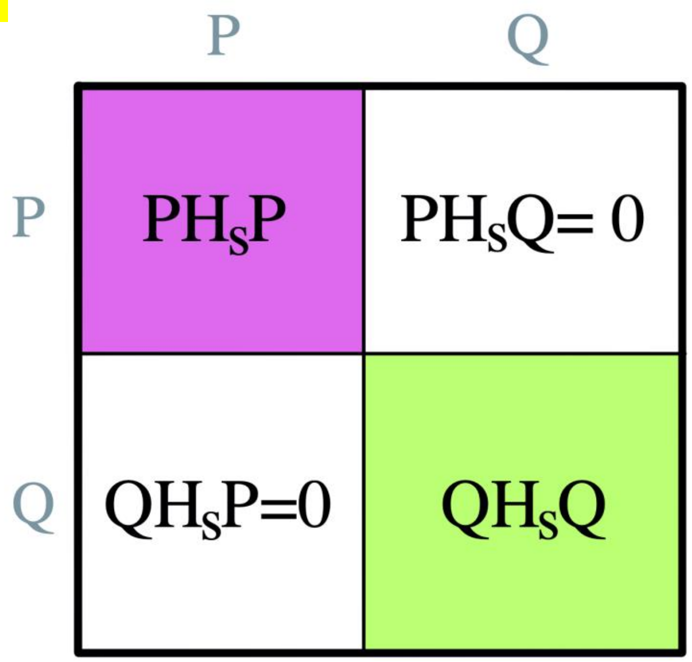

Fig. 3.13 Schematic illustration of two types of RG evolution for NN interactions in momentum space: **a** $V_{\text{low}-\text{k}}$ running in Λ, and **b** SRG running in λ. Here, q and q' denote the relative momenta of the initial and final state, respectively. At each Λ_i or λ_i, the matrix elements outside of the corresponding blocks or bands are negligible, implying that high- and low-momentum states are decoupled

Lee-Suzuki-Okamoto ST

Fig. 3.15 A schematic representation of the effective Hamiltonian in the Lee-Suzuki-Okamoto renormalization scheme. The Hamiltonian $H_P = PH_SP$ in the active model space is renormalized to take into account the Hamiltonian $H_Q = QH_SQ$ in the complimentary space $Q = 1 - P$ by using the similarity transformation operator S defined in Eq. (3.210). There is no coupling between P and Q spaces in the model Hamiltonian

SSRPA for natural parity states

The transition operators of the spin-independent modes are:

$$F_\lambda^{IS} = \sum r_i^n Y_{\lambda 0}(r_i)$$
$$F_\lambda^{IV} = \sum r_i^n Y_{\lambda 0}(r_i)\tau_z(i) \quad (10)$$

$$B(E_\lambda) = |\sum_{ph} b_{ph}(E_\lambda)|^2 = |\sum_{ph}(X_{ph}^\lambda + (-1)^J Y_{ph}^\lambda)F_{ph}^\lambda|^2$$

Normalization condition

$$\sum_{ph}(|X_{ph}^\nu|^2 - |Y_{ph}^\nu|^2) + \sum_{p_1p_2h_1h_2}(|X_{p_1p_2h_1h_2}^\nu|^2 - |Y_{p_1p_2h_1h_2}^\nu|^2) = n_1 + n_2 = 1$$

TABLE I. The energy moments m_1 and m_{-1} of isoscalar 0^+ and 1^+ transitions obtained by the RPA and SSRPA calculations for ^{16}O and ^{40}Ca with SGII interaction.

	^{16}O		
	0^+		
	RPA	$SSRPA_D$	$SSRPA_F$
m_1	673.876	738.777	724.324
m_{-1}	1.169	1.147	1.169
	2^+		
	RPA	$SSRPA_D$	$SSRPA_F$
m_1	8375.433	9831.163	9425.072
m_{-1}	19.471	18.176	19.471
	^{40}Ca		
	0^+		
	RPA	$SSRPA_D$	$SSRPA_F$
m_1	2879.917	3156.741	3091.711
m_{-1}	6.441	6.292	6.441
	2^+		
	RPA	$SSRPA_D$	$SSRPA_F$
m_1	35934.411	39329.832	38566.354
m_{-1}	120.915	116.860	120.915

Self-consistent HF+SSRPA model with Skyrme EDFs

RPA matrices are renormalized taking into account an enlarged model space from 1p-1h to 1p-1h+2p-2h configurations

Convergence check

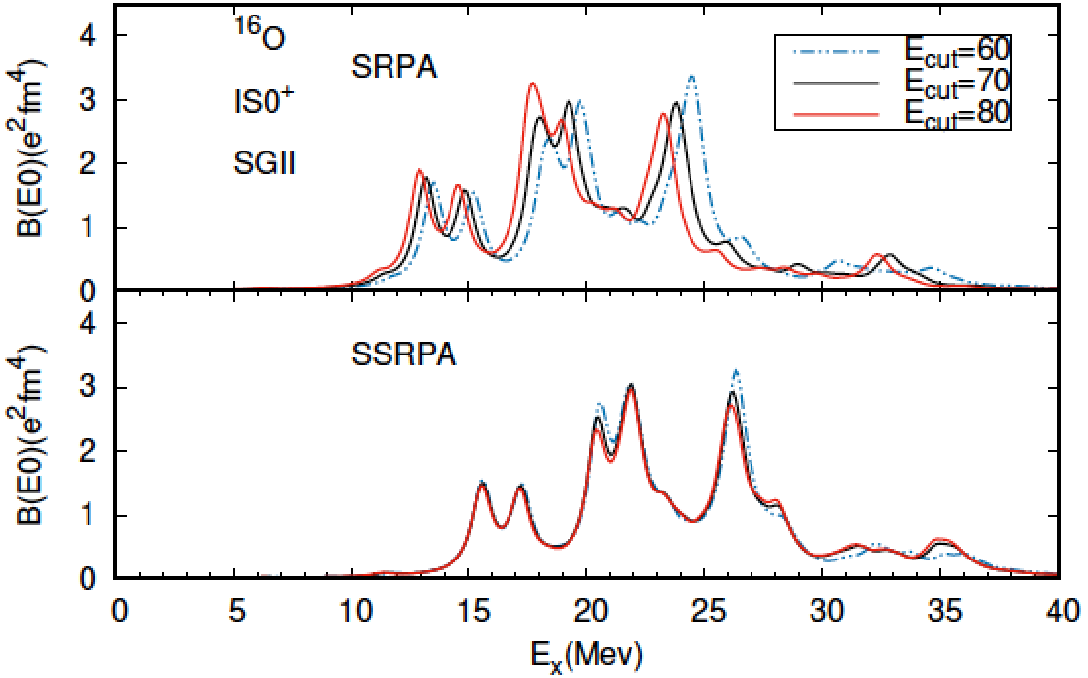

FIG. 1: IS 0^+ strength distributions for ^{16}O calculated by SRPA (upper panel)and SSRPA (lower panel) by SGII interaction with 2p-2h energy cutoff 60, 70, and 80 MeV. See the text for more details.

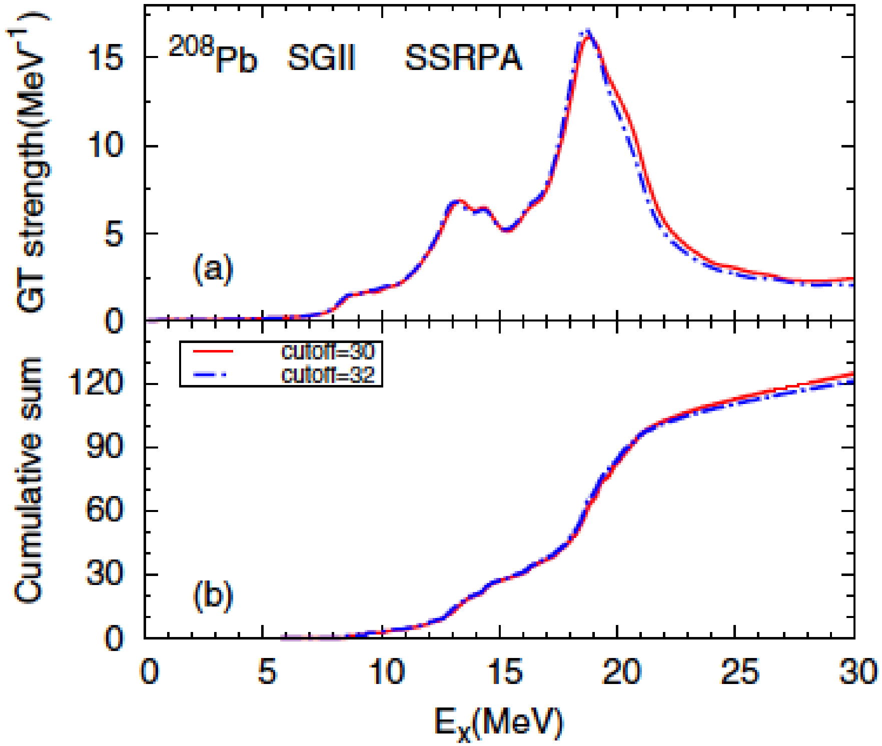

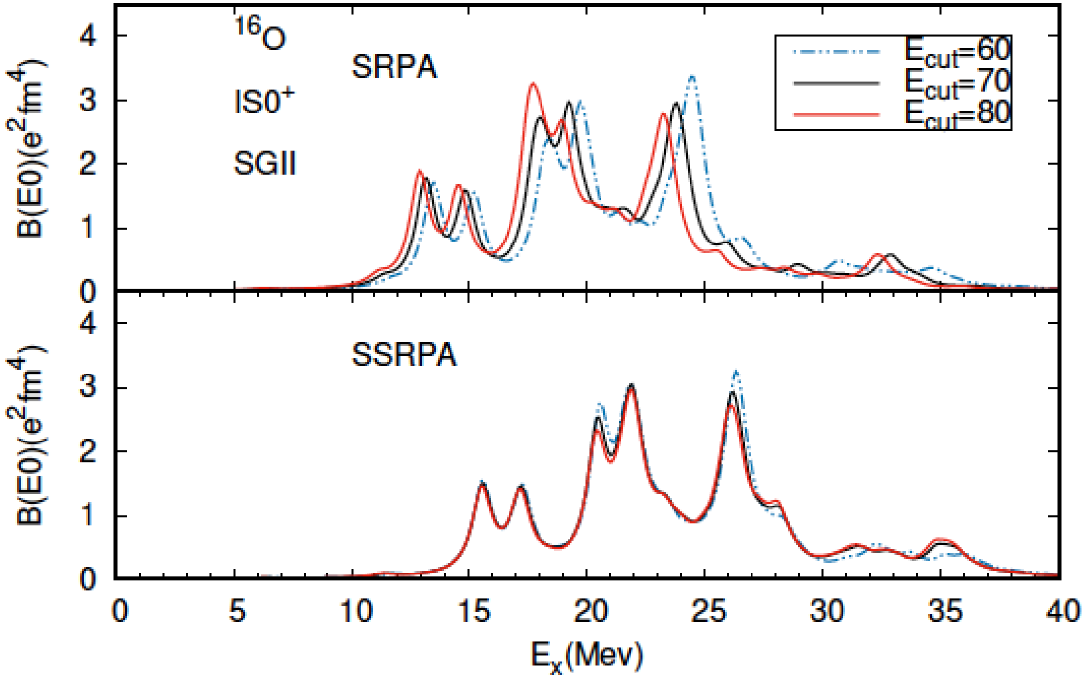

FIG. 1: IS 0^+ strength distributions for ^{16}O calculated by SRPA (upper panel)and SSRPA (lower panel) by SGII interaction with 2p-2h energy cutoff 60, 70, and 80 MeV. See the text for more details.

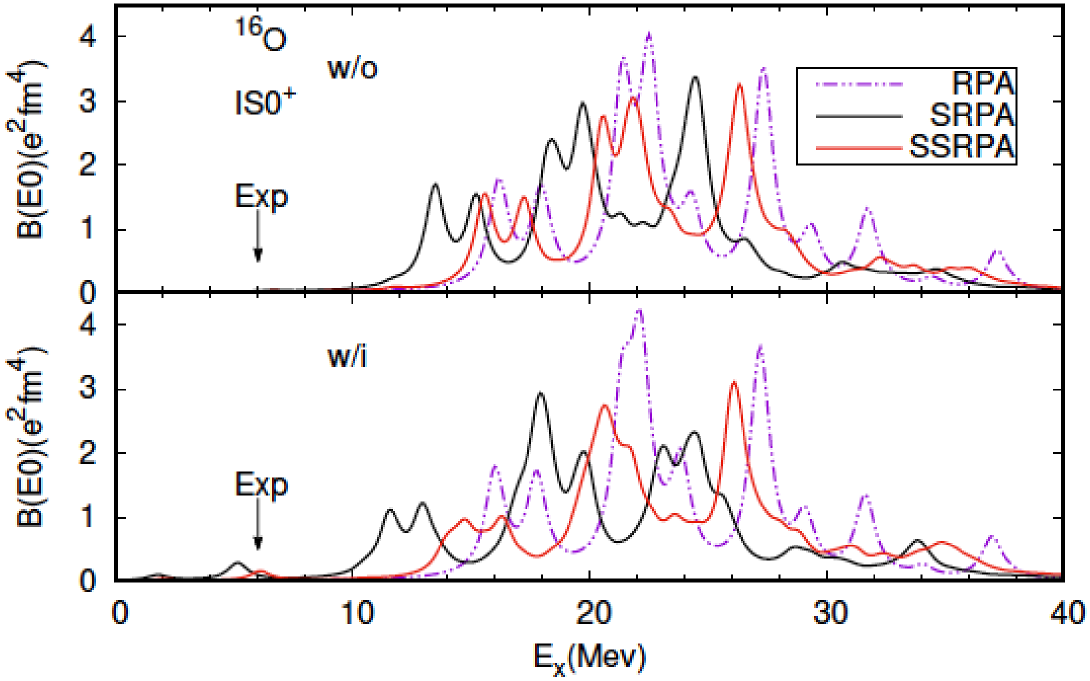

FIG. 2: IS 0^+ strength distributions in ^{16}O. The results calculated without and with tensor interaction are shown in the upper and lower panels, respectively. Results of RPA, SRPA, and SSRPA are labelled by purple dash lines, black solid lines, and red solid lines, respectively. The lowest state measured by experiment [3] is represented by an arrow.

Effects of the Skyrme tensor force on 0^+, 2^+, and 3^- states in ^{16}O and ^{40}Ca nuclei with second random phase approximation

M. J. Yang,[1] C. L. Bai,[1] H. Sagawa,[2] and H. Q. Zhang[3]

[1] *College of Physics, Sichuan University, Chendu 610065, China*
[2] *Center for Mathematics and Physics, University of Aizu, Aizu-Wakamatsu, Fukushima 965-8560, Japan*
RIKEN, Nishina Center, Wako, Saitama, Japan
[3] *China Institute of Atomic Energy, Beijing 102413, China*

PHYSICAL REVIEW C 103, 054308 (2021)

PHYSICAL REVIEW C **106**, 014319 (2022)

Gamow-Teller transitions in magic nuclei calculated by the charge-exchange subtracted second random-phase approximation

M. J. Yang,[1] C. L. Bai,[1] H. Sagawa,[2,3] and H. Q. Zhang[4]

Effects of two particle-two hole configurations and tensor force on β decay of magic nuclei

M. J. Yang,[1] H. Sagawa,[2,3] C. L. Bai,[1] and H. Q. Zhang[4]

[1] *College of Physics, Sichuan University, Chendu 610065, China*
[2] *Center for Mathematics and Physics, University of Aizu, Aizu-Wakamatsu, Fukushima 965-8560, Japan*
[3] *RIKEN, Nishina Center, Wako 351-0198, Japan*
[4] *China Institute of Atomic Energy, Beijing 102413, China*

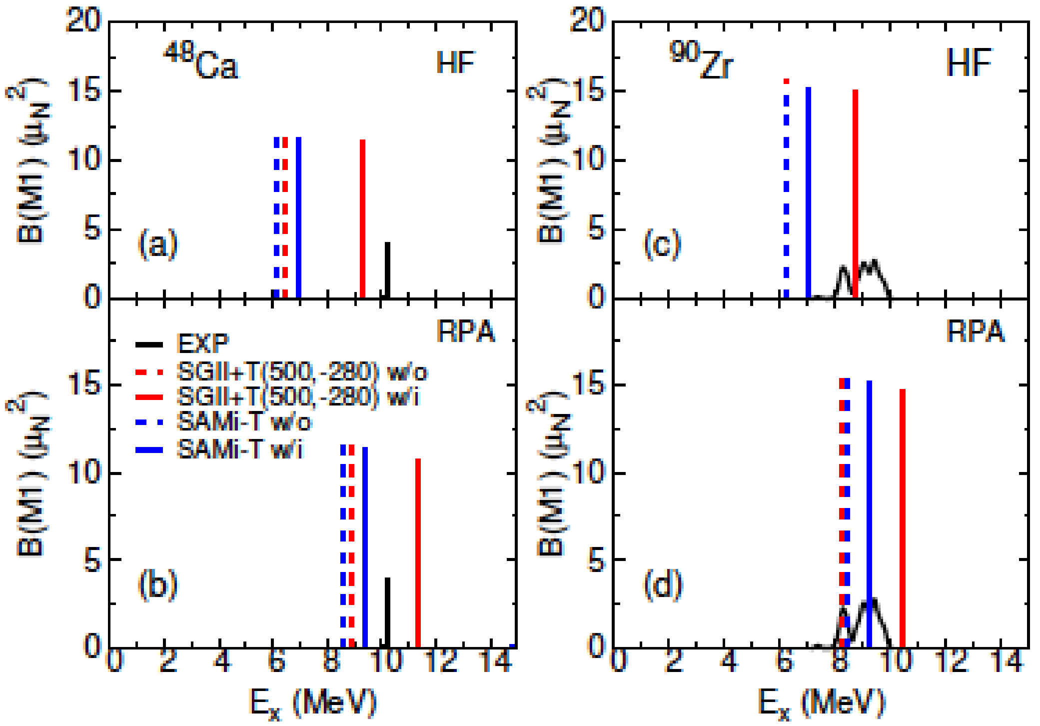

FIG. 1: (Color online) Unperturbed *p-h* and RPA Strength distributions of ^{48}Ca (left panels) and ^{90}Zr (right panels) of M1 states calculated with the SGII+T(500,-280) and SAMi-T (415.5, -95.5) EDFs. The unperturbed *p-h* results are shown in upper panels, while RPA results are shown in lower panels. The results obtained by SGII+T and SAMi-T are shown by red and blue lines, respectively. The experimental data [25] are shown by the black lines. See the text for details.

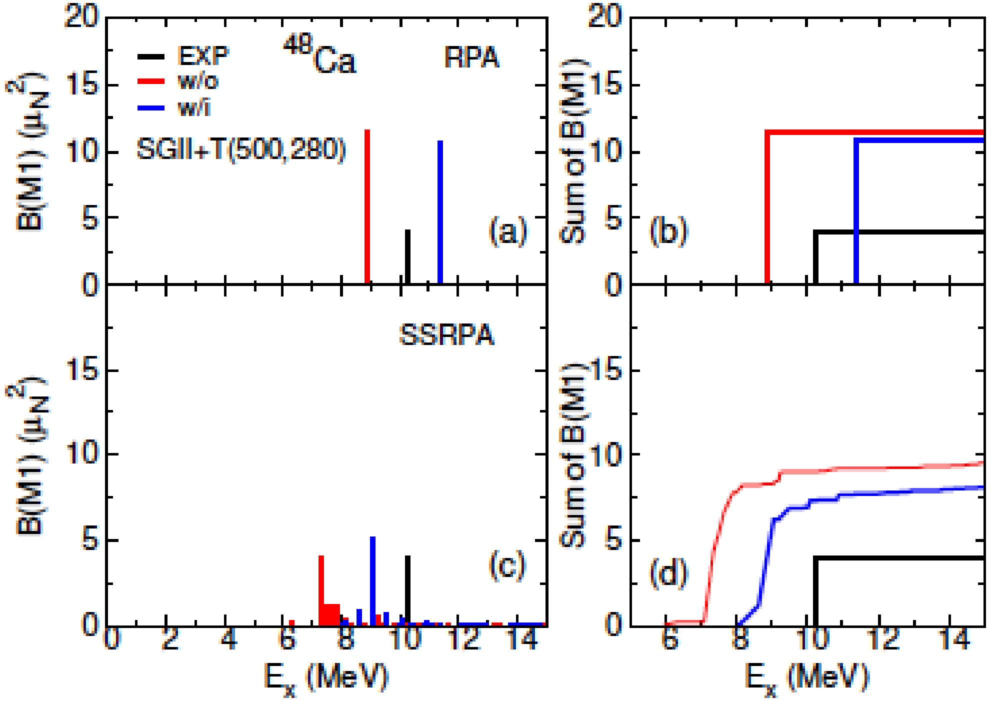

FIG. 2: (Color online) Strength distributions (left panels) and corresponding cumulative sums (right panels) of M1 excitations in ^{48}Ca calculated with the SGII, SGII+T(500,-280) EDFs by RPA (upper panels) and SSRPA (lower panels). The results obtained by SGII and SGII+T(500,-280) are shown by red and blue lines, respectively. The experimental data [25] are shown by the black lines. See the text for details.

Magnetic dipole transitions by SSRPA

T=500 MeVfm^5
U=-280MeVfm^5

TABLE II: The same as Table I, but for ^{90}Zr. The experimental excitation energy is ~9.0 MeV.

SGII	HF	RPA	ΔE(RPA-HF)	SSRPA	ΔE(SSRPA-HF)
w/o	6.21	8.23	2.02	6.81	0.60
with	8.77	10.46	1.69	8.27	−0.50
Δ E^T	1.56	2.23		1.46	
SAMi-T	**HF**	**RPA**	**ΔE(RPA-HF)**	**SSRPA**	**ΔE(SSRPA-HF)**
w/o	6.25	8.42	2.17	7.52	1.27
with	7.05	9.19	2.14	8.20	1.15
Δ E^T	0.80	0.77		1.68	

TABLE III: The main peaks and sums of B(M1) in ^{48}Ca calculated by RPA and SSRPA with the SGII, SGII+T ($T = 500, U = -280$), SGII+Te1 ($T = 500, U = -350$), and SAMi-T ($T = 415.45, U = -95.53$) EDFs including with and without tensor terms. The sums of B(M1) are added up to E_{max}=15 MeV in consistent with those of Fig. 2. The experimental data are taken from Refs. [22–26].

		E_x(MeV)	B(M1) (μ_N^2)	$\sum$ B(M1) (μ_N^2
Expt.	[22]	10.227	4.0±0.3	4.0±0.3
	[23]	10.23	3.9±0.3	5.3±0.6
	[24]	10.23	6.8±0.5	6.8±0.5
	[25]	10.23	3.85±0.32	3.85±0.32
	[26]	10.23	3.85±0.32	5.36±0.49
SGII	RPA	8.90	11.47	11.47
	SSRPA	7.34	4.09	9.54
SGII	RPA	11.35	10.73	10.73
+T(500,-280)	SSRPA	9.05	5.06	8.10
SGII	RPA	11.89	10.49	10.49
+Te1(500,-350)	SSRPA	9.53	2.46	7.75
SAMi-T w/o	RPA	8.60	11.53	11.53
	SSRPA	7.88	3.96	10.21
SAMi-T w/i	RPA	9.40	11.33	11.33
	SSRPA	8.33	6.56	10.06

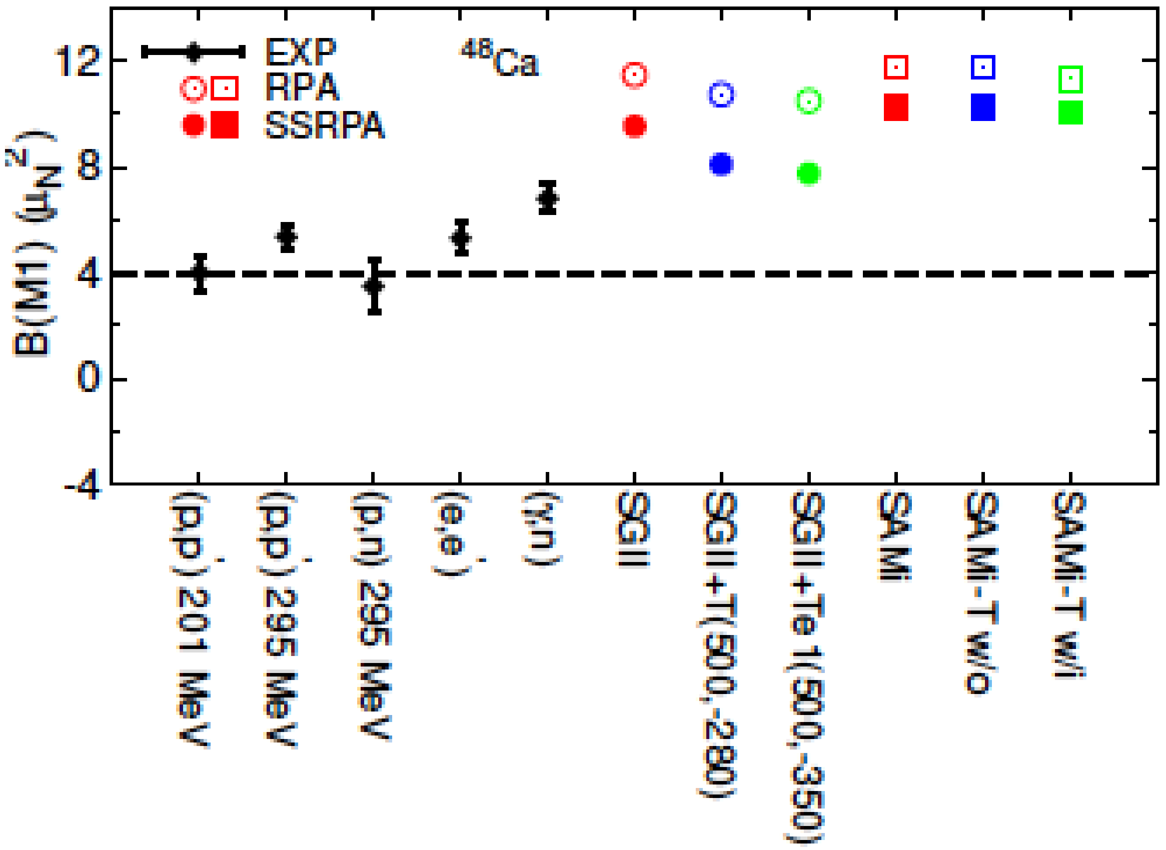

TABLE III: The excitation energy of 1^+ state in ^{90}Zr. The energy is calculated with SGII+(T,U)=(500,-280) and SAMi-T,(T,U)=(415.5,−91.4). Δ E^T is the difference of energy between with and without the tensor interaction. The experimental energy is ∼9.0 MeV. The unit is in MeV.

Excitation Energy

SGII+(T,U)	HF	RPA	ΔE(RPA-HF)	SSRPA	ΔE(SSRPA-HF)
w/o	6.21	8.23	2.02	6.81	0.60
with	8.77	10.46	1.69	8.27	−0.50
Δ E^T	2.56	2.23		1.46	
SAMi-T+(T,U)	HF	RPA	ΔE(RPA-HF)	SSRPA	ΔE(SSRPA-HF)
w/o	6.25	8.42	2.17	7.52	1.27
with	7.05	9.19	2.14	8.20	1.15
Δ E^T	0.80	0.77		1.68	

B(M1) strength

SGII+(T,U)	HF	RPA	SSRPA
w/o	15.53	15.24 (98.1%)	12.56 (80.9%)
with		14.73 (94.8%)	10.93 (70.4%)
ΔB^T		-0.51 (3.2 %)	-1.63 (10.5 %)
SAMi-T+(T,U)	HF	RPA	SSRPA
w/o	15.53	15.37 (99.1%)	13.27 (85.4%)
with		15.22 (98.0%)	13.05 (84..0%)
ΔB^T		-0.15 (1.1%)	-0.22 (1.4%)

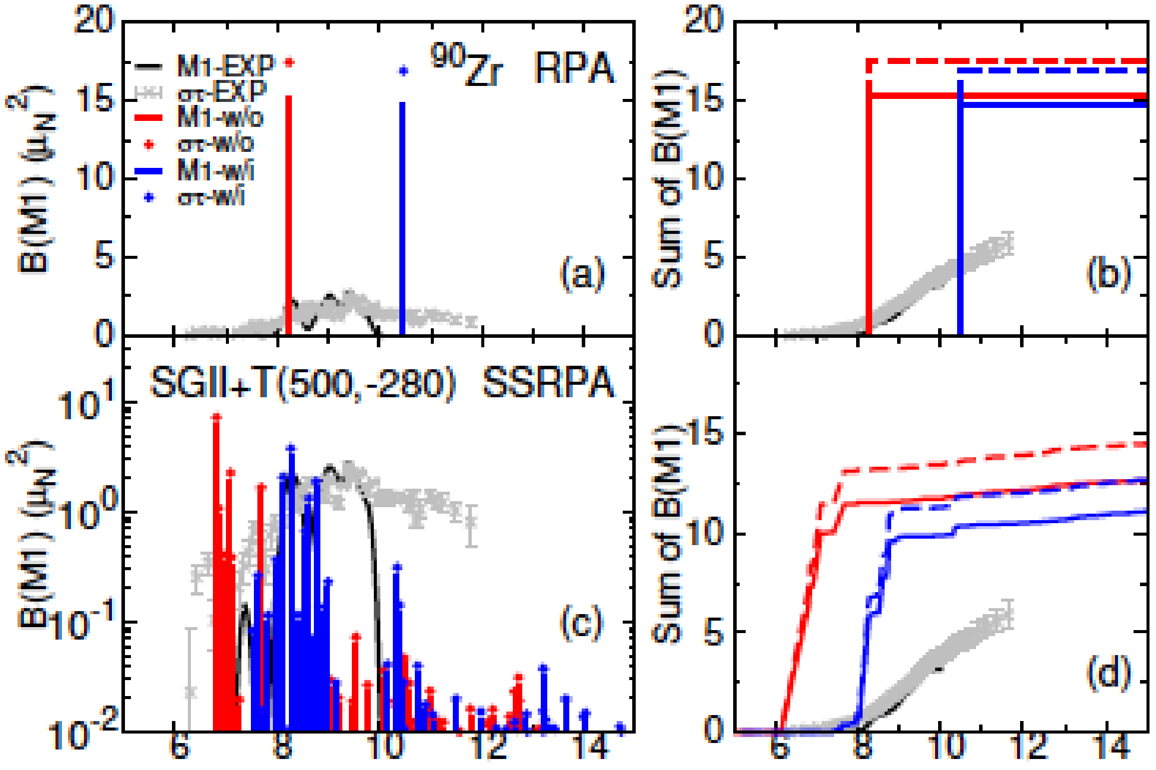

$A = \pi r^2$

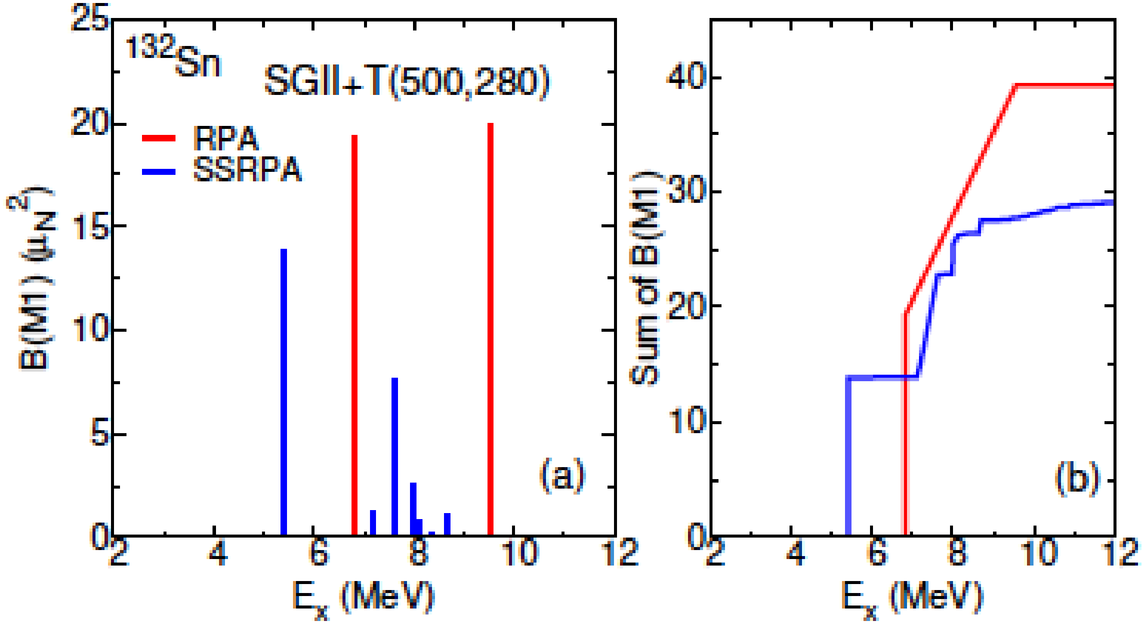

TABLE IV: The same as Table III, but for ^{90}Zr. When the calculated strengths are fragmented in several states in SS-RPA, the theoretical excitation energies are defined by the centroid energies of the strength distributions. The experimental data are from Refs. [27–30].

		E_x(MeV)	$\sum B(M1)$ (μ_N^2)
Expt.	[27]	8.90±0.15	–
	[28]	8.1−10.5	6.7
	[29]	9.53±0.06	–
	[30]	9.0	4.17±0.56
SGII	RPA	8.23	15.24
	SSRPA	7.15	12.56
SGII	RPA	10.46	14.73
+T(500,-280)	SSRPA	8.55	10.94
SGII	RPA	10.93	14.55
+Te1(500,-350)	SSRPA	8.74	10.44
SAMi-T w/o	RPA	8.42	15.37
	SSRPA	7.64	13.27
SAMi-T w/i	RPA	9.19	15.22
	SSRPA	8.30	13.05

[29] C. Iwamoto et al., PRL108,262501 (2012)

$$B(\tau\sigma) = \tau\sigma$$
$$B(M1) = g_l l + g_s s$$

Summary

EDF is optimized for the mean field descriptions of ground states and excited states; HF and RPA level

Second RPA and similar theoretical models beyond mean field should take care of renormalization of EDF which includes already the effect of 1p-1p model space.

Lee-Suzki-Okamoto similarity transformation gives a guide to construct appropriate EDF for beyond RPA models

Progress of Theoretical Physics, Vol. 64, No. 6, December 1980

Convergent Theory for Effective Interaction in Nuclei*)

Kenji SUZUKI and Shyh Yuan LEE*

§ 2. Similarity transformation and Rayleigh-Schrödinger theory

We consider a many-body system which is described by the Schrödinger equation

$$H|\Psi\rangle = E|\Psi\rangle \tag{2·1}$$

with the Hamiltonian

$$H = H_0 + V\ , \tag{2·2}$$

P:1p-1h
Q:2p-2h+---

$$[H_0, P] = [H_0, Q] = 0\ ,$$

$$QH_0P = PH_0Q = 0\ .$$

a similarity transformation

$$X = e^{\omega},$$

$$\mathcal{H} = e^{-\omega} H e^{\omega},$$

ω is an operator which has the properties

$$\omega = Q\omega P\ ,$$

$$P\omega P = Q\omega Q = P\omega Q = 0\ .$$

the effective Hamiltonian $H_{\rm eff}$ is given by

$$H_{\rm eff} = P\mathcal{H}P = P(X^{-1}HX)P\ .$$

$$H_{\rm eff}|\phi\rangle = \mathcal{H}|\phi\rangle$$